Mon. Not. R. Astron. Soc. **000**, 1–9 (2013) Printed 30 March 2015 (MN LATEX style file v2.2)

Reducing noise in moving-grid codes with strongly-centroidal Lloyd mesh regularization

Philip Mocz[1⋆], Mark Vogelsberger[2], Rüdiger Pakmor[3], Shy Genel[4]†, Volker Springel[3,5], Lars Hernquist[1]

[1]*Harvard-Smithsonian Center for Astrophysics, 60 Garden Street, Cambridge, MA 02138, USA*
[2]*Department of Physics, Kavli Institute for Astrophysics and Space Research, Massachusetts Institute of Technology, Cambridge, MA 02139, USA*
[3]*Heidelberger Institut für Theoretische Studien, Schloss-Wolfsbrunnenweg 35, 69118 Heidelberg, Germany*
[4]*Department of Astronomy, Columbia University, 550 West 120th Street, New York, NY 10027, US*
[5]*Zentrum fr Astronomie der Universitt Heidelberg, Astronomisches Recheninstitut, Mnchhofstr. 12-14, 69120 Heidelberg, Germany*

submitted to MNRAS, Mar 2015

ABSTRACT

A method for improving the accuracy of hydrodynamical codes that use a moving Voronoi mesh is described. Our scheme is based on a new regularization scheme that constrains the mesh to be centroidal to high precision while still allowing the cells to move approximately with the local fluid velocity, thereby retaining the quasi-Lagrangian nature of the approach. Our regularization technique significantly reduces mesh noise that is attributed to changes in mesh topology and deviations from mesh regularity. We demonstrate the advantages of our method on various test problems, and note in particular improvements obtained in handling shear instabilities, mixing, and in angular momentum conservation. Calculations of adiabatic jets in which shear excites Kelvin Helmholtz instability show reduction of mesh noise and entropy generation. In contrast, simulations of the collapse and formation of an isolated disc galaxy are nearly unaffected, showing that numerical errors due to the choice of regularization do not impact the outcome in this case.

Key words: methods: numerical – hydrodynamics – MHD

1 INTRODUCTION

New computational methods for fluid dynamics that employ a moving Voronoi mesh approach have been developed in the past several years to simulate astrophysical and cosmological systems. Codes based on this method include AREPO (Springel 2010), which has recently been used to run the 12 billion resolution element state-of-the-art "Illustris" cosmological simulation (Vogelsberger et al. 2014a,b; Genel et al. 2014), TESS (Duffell & MacFadyen 2011), adapted for relativistic hydrodynamics, the moving mesh algorithm presented in Gaburov, Johansen & Levin (2012) for the simulation of magnetically levitating accretion disks around supermassive black holes, and the RICH code (Steinberg et al. 2015). The moving Voronoi framework has also been extended to finite-element techniques (Mocz et al. 2014) and constrained transport approaches for magnetohydrodynamics (MHD) to strictly maintain the divergence-free nature of the magnetic field (Mocz, Vogelsberger & Hernquist 2014). Related mesh-free methods have also been developed by Hopkins (2014), which use Riemann solvers acting over volume "overlaps", and have similar advantages to the moving mesh approach, and have particularly good angular momentum conservation but at the cost of enhanced noise.

Moving mesh codes have found success due to the numerical advantages they provide because of their quasi-Lagrangian nature, Galilean-invariant formulation (for non-relativistic fluids), limited advection errors, preservation of contact discontinuities, continuous spatial adaptability, and ability to accurately resolve instabilities. Notably, the moving mesh method provides advantages over previous smoothed particle hydrodynamics (SPH) approaches, which can suppress entropy generation by mixing, underestimate vorticity generation in curved shocks, prevent efficient gas stripping from infalling substructures (Sijacki et al. 2012), and have relatively poor convergence properties (e.g. Zhu, Hernquist & Li 2015); and also over adaptive mesh refinement (AMR) codes, which can have large advection errors due to numerical diffusion in the presence of large supersonic bulk velocities.

However, moving Voronoi mesh codes can be affected by noise on small spatial scales due to the mesh motion (Bauer & Springel 2012; Hopkins 2014). As the mesh evolves, the orientation and sizes of the faces and the topology of the connections between cells change, introducing small truncation errors in the solution, which can lead to artificial additional power on the smallest scales (Bauer & Springel 2012) and numerical secondary instabil-

⋆ E-mail: pmocz@cfa.harvard.edu (PM)
† Hubble Fellow

ities in shear flows. The errors are largest in the presence of shear, when the mesh cells move past each other and change face boundaries rapidly, because the standard moving mesh formulations assume that the face orientations do not evolve significantly in one timestep or may not adequately capture rapid changes. If the mesh generating points strictly move with the fluid velocity, the mesh noise can be quite large because the Voronoi cells can deform into highly irregular shapes.

Mesh regularization, i.e., applying a small correction to the mesh generating points of the cells in a way that keeps the cells "well-behaved" (round and centroidal) provides a handle on this error. The mesh generating points travel with the fluid velocity plus some small correction to keep the mesh approximately regular and centroidal. The approach taken by Springel (2010) adds a small correction in the direction of the center-of-mass at the beginning of the time step (or sub time step in the case of higher-order time integration). Vogelsberger et al. (2012) modify this approach for cosmological simulations by considering the maximum opening angle of a face at the mesh generating point and the density gradient direction to set the correction. The correction term scales as the sound-speed inside the cell, which ensures a timestep independent formulation. We will refer to this class of regularization methods as sound-speed regularization (SSR).

Despite keeping the cells approximately regular, these techniques do not eliminate mesh noise entirely because there are several small sources of error present in the formulation. First, the motion of the mesh generating points (and hence the change in the orientation of the faces) is not smooth. The direction of the correction only takes into account the geometry at the beginning of the time step. After the mesh advances to the next timestep, a small offset between the mesh generating point and the center-of-mass remains, which may point in an uncorrelated direction from that at the beginning of the time step. The cell then obtains an small kick in that uncorrelated direction, adding a small level of random noise to the smooth mesh deformation. Second, a small offset exists in the center-of-mass and mesh generating point. This causes the cells to have some spin about their center of mass, and also introduces errors in the second-order estimates of cell gradients (Springel 2010), which assumes the two points coincide. This later issue has recently been resolved in Pakmor et al. (2015), where an improved least-squares-fit gradient estimator has been developed that can achieve second-order accuracy for smooth flows.

Recently, Duffell & MacFadyen (2014) proposed a smoothing of the velocities of the mesh generating points to alleviate the problem of mesh noise. Their scheme exhibits a reduction in: grid noise, numerical secondary instabilities, and artificial power in the power-spectrum of the solution field on the smallest spatial scales (although not at the level of fixed grid codes). The smoothing method overcomes the issue of the uncorrelated randomly directed corrections that violate a fully smooth mesh motion. However, setting the cell vertex velocities to the fluid velocity and smoothing by the neighbours does not enforce a strongly centroidal mesh (only approximately centroidal; as do the other regularization methods in the literature); deviations from a centroidal mesh introduce errors in e.g. Green-Gauss gradient estimates. Moreover, in the presence of shear flows, the cell velocities in this approach will be smoothed out, reducing the code to a static mesh code, and thus losing the desired properties of a moving mesh code such as advecting the solution at high precision.

We have developed a new regularization scheme to address the smoothness and strong-centroidality issues, which is presented here. We refer to the method as strongly-centroidal Lloyd regularization (LR). Our approach evolves the mesh in a smooth, centroidal manner. Unlike the previous techniques, it accounts for where the center-of-mass of a cell travels to at the *end* of a time step in order to ensure the centroidal property, making it in essence a forward-predicting, iterative Lloyd's algorithm. The concept is straightforward. The velocities of mesh generating points are initialized to the values of the local fluid velocity, and a few iterations of corrections are applied to modify this velocity so that the cell moves to the location of its center-of-mass at the end of the time step. This results in a smoothly evolving centroidal Voronoi mesh that moves approximately with the fluid velocity. The scheme may optionally be modified to a weighted centroidal scheme (weighted by the fluid density) for simulations with collapsing structure to gain automatic increased resolution in regions of high density. We demonstrate significant reduction of mesh noise with the new regularization scheme.

Developing reliable numerical codes that offer general adaptability to a huge spatial and temporal dynamic range is an ongoing challenge. Recently Pakmor et al. (2015) have improved the accuracy and angular momentum conservation for moving-mesh codes by developing new time integration scheme and spatial gradient estimates in the AREPO code, significantly improving the precision of the code in smooth test problems. In that work, the MUSCL-Hancock (MH) scheme (Toro 1999) is replaced by a second-order, time symmetric Runge-Kutta (RK) integrator via Heun's method. Additionally, the Voronoi-improved Green-Gauss (GG) gradient estimates are replaced by a least-squares gradient estimator (LSF). Our regularization complements these recent improvements for smooth flows by improving the accuracy of moving mesh algorithms when shear is present.

We describe the method and its computationally efficient implementation in Section 2. Several numerical tests are performed to show the advantages of our approach, the results of which are presented in Section 3. We offer concluding remarks in Section 4.

2 STRONGLY-CENTROIAL LLOYD REGULARIZATION

The regularization scheme involves initially setting the velocity of the mesh generating point $\mathbf{w}_i$ of each cell i equal to the local fluid velocity $\mathbf{v}_i$:

$$\mathbf{w}_{i,0} = \mathbf{v}_i \tag{1}$$

Then, in each successive iteration J, the predicted locations of the centers-of-mass of the cells $\tilde{\mathbf{c}}_{i,J}$ are computed at the end of the timestep Δt, and the mesh generating point velocities are updated to:

$$\mathbf{w}_{i,J} = \left(\tilde{\mathbf{c}}_{i,J} - \mathbf{r}_i\right)/\Delta t \tag{2}$$

where $\mathbf{r}_i$ is the location of cell i at the beginning of the timestep.

This iteration is essentially a Lloyd's algorithm for converging an arbitrary Voronoi diagram to a centroidal one. We take 5 iterations in the simulations shown, as the method quickly produces a strongly centroidal mesh. We have explored this free parameter and found that 2 iterations is sufficient to produce quantitatively very similar results.

Optionally, a limiter on the magnitude of the correction to the velocity may be added to explicitly enforce the motion of the mesh generating particles to be close to Lagrangian. We propose the following, Galilean-invariant limiter, based on the local sound speed

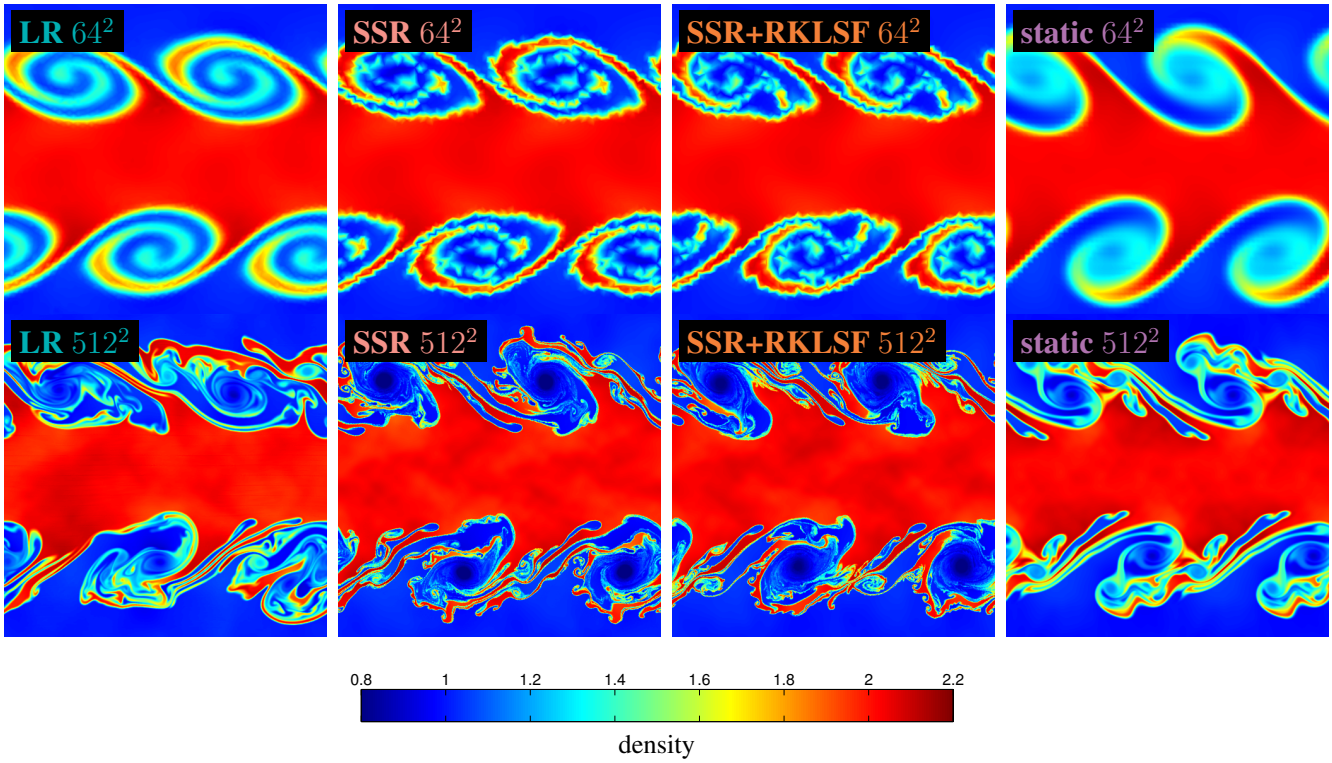

Figure 1. Comparison of KHI with the new (LR) and previous (SSR) regularization schemes at low and high resolution at $t = 2.0$. LR eliminates secondary numerical instabilities, which are present in the simulations that use SSR, even with the recent RK and LSF improvements. For comparison, runs on a static grid are also shown, which also do not have secondary numerical instabilities.

$c_{s,i}$ of the cell.

$$\tilde{\mathbf{c}}_{i,J} \leftarrow (\mathbf{r}_i + \Delta t \mathbf{w}_{i,0}) + (\tilde{\mathbf{c}}_{i,J} - (\mathbf{r}_i + \Delta t \mathbf{w}_{i,0})) \times \min\left(1, \frac{f c_{s,i} \Delta t}{\|\tilde{\mathbf{c}}_{i,J} - (\mathbf{r}_i + \Delta t \mathbf{w}_{i,0})\|}\right) \quad (3)$$

That is, we restrict the motion of the cell to remain within a circle of radius $f c_{s,i} \Delta t$, $(0 < f < 1)$ around the first predicted location of the mesh vertex (which is just predicted by the fluid velocity).

The scheme may also be modified so that the centers-of-mass $\tilde{\mathbf{c}}_{i,J}$ are calculated by weighting with the density field, to bias the movement of the cells to regions of high density. Alternatively, for a simpler implementation with the same effect, the initial velocities in Equation 1 may be biased by a density gradient term as in Vogelsberger et al. (2012), to move cells together towards regions of collapse.

An efficient implementation of the method does not require new mesh reconstruction in each iteration. The center-of-mass of cell i in the predictive step may be calculated by just using the points that are neighbours of the cell at the beginning of the timestep (kicking them forward in time to build the predictive Voronoi cell). This strategy avoids additional in-circle tests. In cases where the mesh topology changes, this is not strictly an exact calculation of the center-of-mass, but the error is negligible since a Voronoi diagram changes continuously.

3 NUMERICAL TESTS

3.1 Reduction of artificial secondary instabilities in the Kelvin Helmholtz instability

As a first test, we demonstrate how the mixing and formation of secondary instabilities in the Kelvin Helmholtz instability (KHI) changes visibly from the original KHI tests that were presented in the AREPO paper (Springel 2010) using SSR. The setup of the initial conditions of this shear flow is described in Springel (2010). The evolved KHI at $t = 2.0$ is presented in Fig. 1 with both the LR and SSR schemes, at low and high resolutions. With the LR approach, we have enforced near-Lagrangian motion with the correction limiter parameter of $f = 0.1$. We ran the LR simulation with the old MH integrator and the GG gradient estimates. For comparison, we ran the SSR simulation in the MH integrator and GG gradient estimates mode, as well as the new RK integrator and LSF gradient estimates mode.

The SSR scheme shows evidence of mesh noise at both low and high resolutions; there is structure present on the scale of the mesh size, at either resolution. The LR method produces a result that is smooth and in agreement with high resolution fixed-grid simulations in terms of the secondary instabilities that develop (c.f. the static mesh runs shown for comparison in Fig. 1, or the static mesh runs in Fig. 34 of Springel (2010), or the static mesh finite-element simulations in Fig. 8 of Mocz et al. (2014)). Small scale secondary instabilities that are present with the SSR scheme disappear with the new LR method. The density field can be said to be well-resolved with the LR technique because there are no structures on the length scale of the cell size. It is worth pointing out that the solution is not exactly symmetric at high resolution because truncation errors lead to chaotic behaviour. We claim the secondary in-

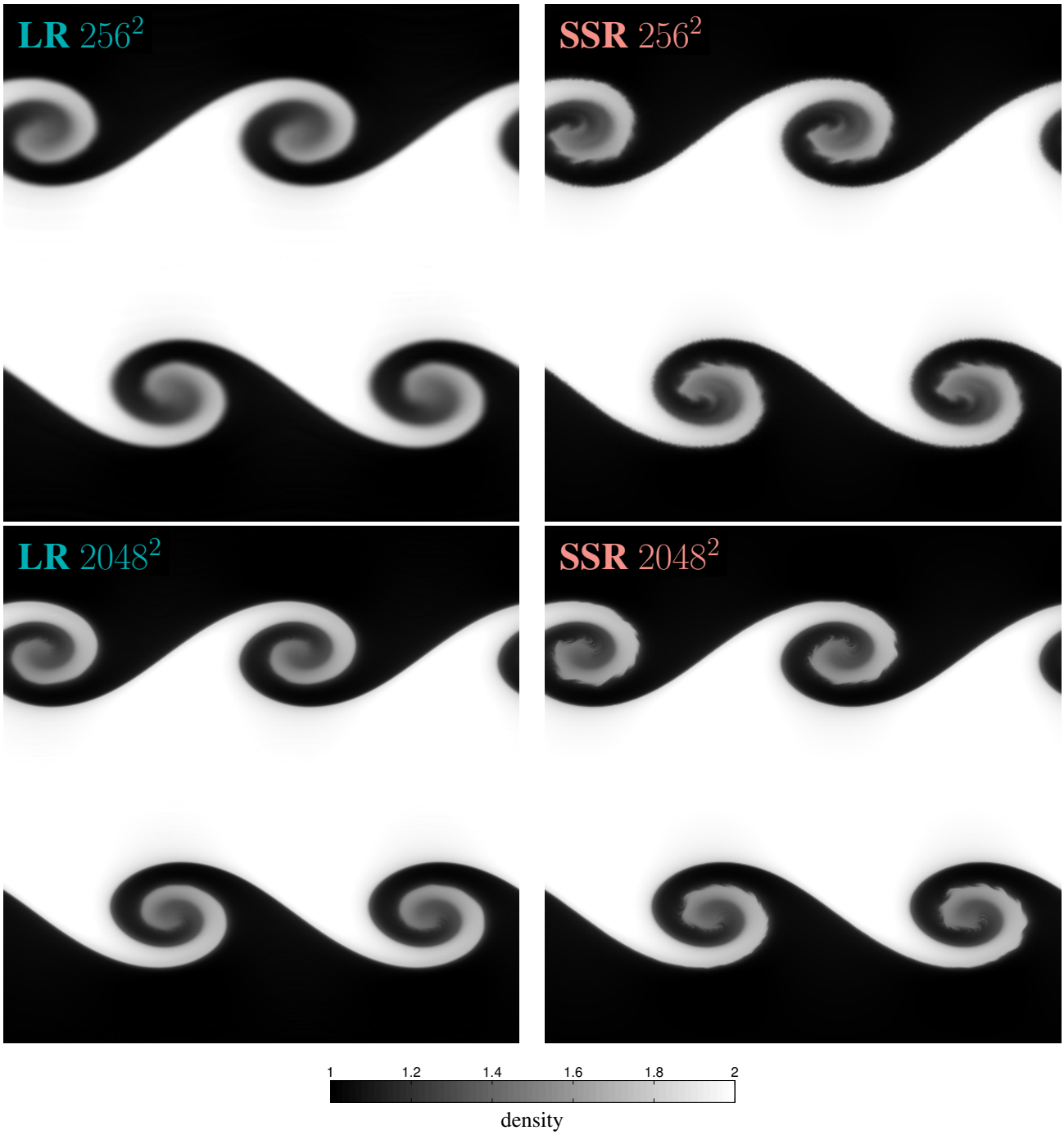

Figure 2. Comparison of KHI with the SSR and LR schemes at low and high resolution. The LR scheme eliminates secondary numerical instabilities.

stabilities present in the old SSR scheme runs are purely numerical artifacts, which we demonstrate below with a second KHI test.

We investigate the KHI setup of McNally, Lyra & Passy (2012), which is a benchmark test in which only a single mode is excited and analytic theory exists to predict the growth rate. Very high resolution simulations of the instability are performed in McNally, Lyra & Passy (2012) using the 6-th order (in space) finite difference PENCIL code. In Fig. 2, we show that the SSR scheme produces secondary instabilities on the scale of the cell size, which are not present with the LR approach. The growth rate of the primary mode of the instability of this test is still simulated accurately with both regularization methods and agrees with theory, as calculated and presented in Fig. 3; only at late times (in the non-linear regime) are small deviations observed in the growth rate of the instability simulated with the two regularization techniques, where we expect the LR scheme is providing more accurate results due to the suppression of the secondary numerical instabilities.

We explore the Lagrangian nature of the SSR and LR schemes in Fig. 4, where we plot the relative changes in the mass of each cell as a function of time. In a purely Lagrangian scheme, there is no mass exchange between particles. We see that the SSR and LR schemes saturate to the same level of mass exchange, regard-

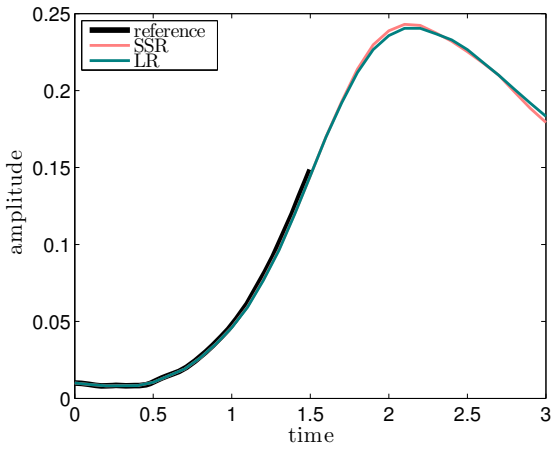

Figure 3. Growth rates of the KHI simulated using the two regularization methods both show good agreement at early times with theory.

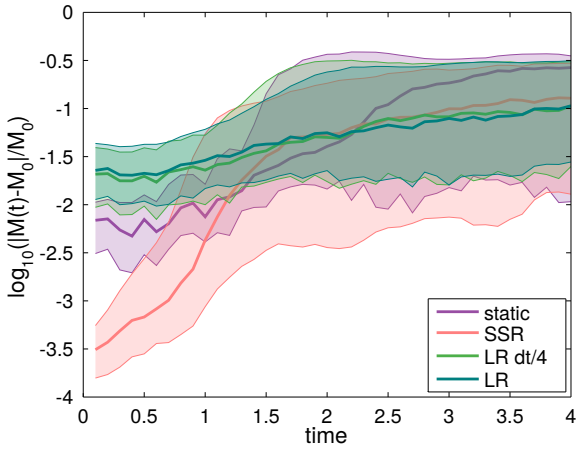

Figure 4. Comparison of the mass of each cell as a function of time in a KHI simulation for the different regularization schemes (static mesh, SSR, LR with $1/4$ the time step, LR). The lines and shaded regions represent the quartiles of the distribution.

less of whether the timestep is decreased by a factor of 4. Hence, we observe no strong implicit dependence of the deviation from Lagrangian behaviour on the time step. We have also explored reducing the number of Lloyd iterations from 5 to 2, and the mass exchange as function of time and the density solution at $t = 2$ do not change noticeably, so they are not shown. The mass exchange on a static mesh saturates to a higher level than the moving mesh approaches due to its Eulerian nature.

3.2 Reduction of noise in the MHD Orszag-Tang Vortex

We next consider simulations of the Orszag-Tang vortex (Orszag & Tang 1979), a common MHD test problem that involves supersonic shocks and decaying turbulence. The setup of the problem is described in detail in Mocz, Vogelsberger & Hernquist (2014). We solve the system using the constrained transport algorithm for a moving mesh described in Mocz, Vogelsberger & Hernquist (2014). The outputs of the simulation at $t = 0.5$ are presented in Fig. 5. The SSR scheme produces numerical noise in the density field, particularly at the locations of shocks and shear flows (compare the center and the shocks in the four cardinal directions in the image). The degree of these numerical noise errors can be changed by altering the mesh regularization parameters of the SSR technique, but it is difficult a priori to predict to what extent. For the tests presented here, we chose the typical values suggested in Springel (2010), and also explored stronger regularization parameters, but found that the noise does not go away completely because the corrections to the mesh generating point locations are not applied in precisely the right directions to keep the cells centroidal to high precision. These numerical artifacts, however, are completely eliminated by the LR scheme, which produces a clean, smooth solution. We note that there are no parameters to adjust in the LR approach: the simulation was run without the optional Lagrangian-enforcer (i.e., $f = \infty$).

In Fig. 5 we tagged cells initially on the $y = 0$ axis at $t = 0$ to show where they finish at the end of the simulation, to demonstrate that both regularization methods move the cells approximately with the fluid flow, as they land approximately in the same places, demonstrating that the scheme is quasi-Lagrangian. Thus, just a tiny correction to the cell vertex velocities can have large implications on the amount of grid noise in the solution: directed at the right orientations they can be used to remove the grid noise almost entirely.

We verify that the LR scheme keeps the mesh regularized to a much higher degree. A histogram of the relative center-of-mass, mesh generating point offset for the two regularization techniques is shown in Fig. 6. The LR method shows over an order of magnitude improvement, and can be arbitrarily improved with more iterations in the regularization algorithm. The offsets in the SSR scheme, on the other hand, can be quite large (> 10 per cent of the cell's effective radius).

3.3 Proper 2nd order convergence in Yee Vortex and Improved Angular Momentum Conservation

With the LR scheme, we can achieve formal second order convergence with a moving Voronoi mesh code, which has been long-standing issue (see also Pakmor et al. (2015) which achieves second order accuracy using an RK integrator and LSF gradient estimates). In many applications second-order convergence is not possible because the astrophysical flows generate shocks, and in the presence of these shocks the slope limiter reduces the order of accuracy to first-order in order to maintain numerical stability across discontinuities. However, second-order convergence should be expected for smooth flows.

We achieve second order convergence by using the LR scheme and the time-symmetric RK integrator (Pakmor et al. 2015) but unlike Pakmor et al. (2015) we can use GG gradient estimates since the mesh remains highly centroidal. The RK integrator averages a flux calculated with the mesh geometry at the beginning and end of the time step, instead of using just the mesh geometry at the beginning of the time step as the original MH integrator of AREPO does. We demonstrate the ability of the code with the new LR scheme to show second-order convergence in the Yee vortex problem, a 2D isentropic, differentially-rotating, steady-state smooth flow (Yee, Sandham & Djomehri 1999).

The flow is described with parameters $T_{\rm inf} = 1$, $\beta = 5$, $\gamma = 1.4$, and box size $L = 10$. The temperature, density, velocity, and

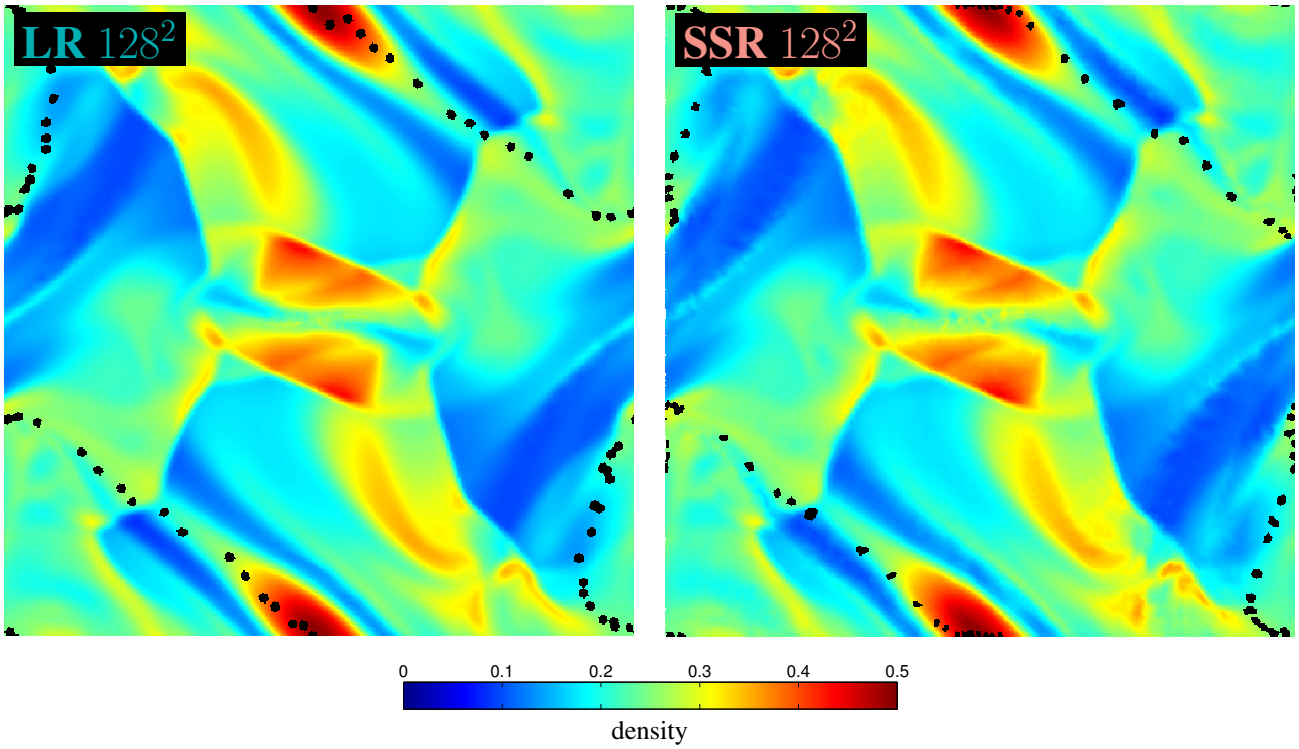

Figure 5. Density field at $t = 0.5$ in the Orszag-Tang vortex simulated with the SSR and LR schemes. The LR scheme eliminates noise at locations of shocks and shear flow in the simulation. A number of cells are tagged in black (initially on the $y = 0$ axis at $t = 0$) to visually verify that they have travelled to similar locations at the end of the simulation.

pressure profiles are given as follows.

$$T(r) = T_{\rm inf} - \frac{(\gamma-1)\beta^2}{8\gamma\pi^2}{\rm e}^{1-r^2} \tag{4}$$

$$\rho(r) = T^{1/(\gamma-1)} \tag{5}$$

$$v_x(r) = -y\frac{\beta}{2\pi}{\rm e}^{(1-r^2)/2} \tag{6}$$

$$v_y(r) = x\frac{\beta}{2\pi}{\rm e}^{(1-r^2)/2} \tag{7}$$

$$P(r) = \rho^\gamma/\gamma \tag{8}$$

We simulated this flow to $t = 10$, a time at which the vortex has differentially rotated several times. Fig. 7 shows a well behaved profile using the LR scheme, but a noisy one with the SSR technique, even with the RK time integrator. We see that due to the presence of this mesh noise, the SSR method is unable to achieve second-order convergence of the L1 norm error of the density profile, as shown in the convergence plot Fig. 8. Beyond some fairly low resolution, the mesh noise dominates the error in this test problem. However, this noise is removed with the LR scheme.

We simulate the flow much longer, up to $t = 100$ to study the long term behaviour of the angular momentum. The L1 norm error of the angular momentum is reduced by an order of magnitude once the LR scheme is added, as shown in Fig. 9, and grows with time in a predictable manner as $t^{0.5}$ for this problem. The angular momentum without the LR scheme can fluctuate unpredictably due to mesh noise, as also shown in Fig. 9. The total angular momentum is well behaved with the LR and RK time integrator improvements, as shown in Fig. 10, while with the original formulation of AREPO it can grow non-linearly, which has previously placed some limitations on the application of moving Voronoi mesh codes like AREPO or TESS for rotationally symmetric accretion flows. With the LR scheme, we have improved the angular momentum conservation of the moving mesh approach, and at the same time reduced the mesh noise.

The well-behaved convergence with LR is achieved because there are no errors in the gradient estimate present that are caused by deviations from a fully centroidal mesh, which again result from the noise in the movement of the mesh-generating points. We emphasise that the combination of GG gradients and a centroidal mesh even guarantees second order accurate gradients, whereas LSF gradients are only first order accurate in general (for a Cartesian mesh, they are also second order).

3.4 Reduction of artificial power in turbulence test

We present the results of 3D subsonic driven turbulence, whose setup is described in Bauer & Springel (2012), and was also presented in Mocz et al. (2014), where the system was investigated using finite-element methods. The energy power spectrum for such a turbulent system is well described by a Kolmogorov power-law on the range of spatial scales that are resolved by the mesh. However, the energy cascade is artificially limited by the sizes of the cells, and there is excess artificial accumulation of energy on these scales. This excess build-up typically has tended to be larger in moving mesh codes than in static mesh codes, with mesh noise being a likely culprit as it adds fluctuations on the length scale of the cell size. In Fig. 11, we show that the artificial accumulation of energy on the scale of the cells is reduced with the LR approach. The LR run used a Lagrangian enforcing parameter of $f = 0.1$, same

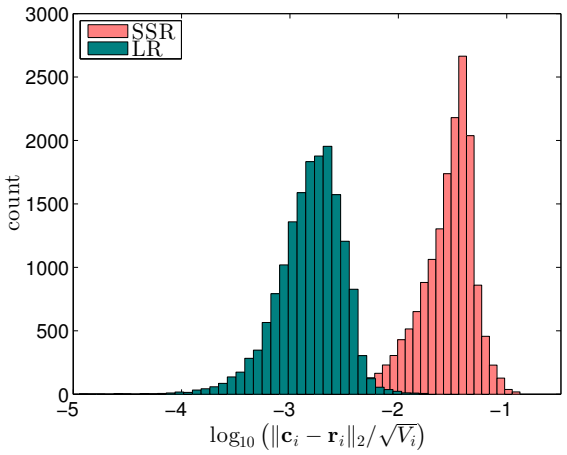

Figure 6. A histogram of the relative center-of-mass, mesh generating point offset for the two regularization methods. The LR scheme shows over an order of magnitude improvement. The errors in the SSR technique can be quite large, > 10 per cent.

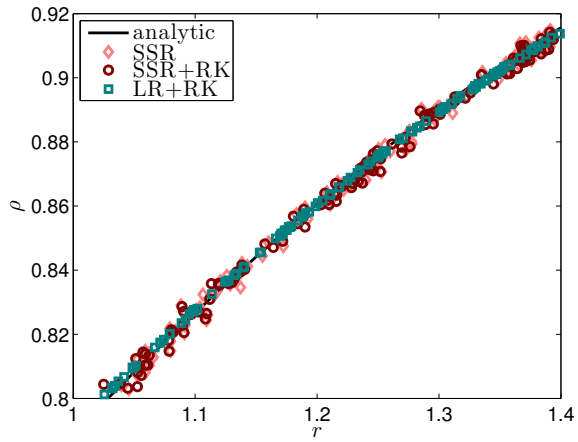

Figure 7. The density profile of the Yee vortex at $t = 10$, with the SSR and time stepping scheme, the RK time stepping scheme, and the RK scheme with the LR method. The LR eliminates the mesh noise.

as the KHI simulations, chosen so that the relative offsets between centres-of-mass and mesh generating points are reduced by at least an order of magnitude from the SSR scheme.

We study the Lagrangian nature of the simulations by adding passive Monte Carlo tracers in the turbulence tests, as in Genel et al. (2013). The number of exchanges between cells, $N_{\rm exch}$, that Monte Carlo tracers experience as a function of time, should be ideally zero in a fully-Lagrangian code. We plot the evolution of this quantity in Fig. 12. The LR and SSR methods show greatly reduced exchanges from a static mesh run, as expected. For a Lagrangian enforcing parameter of $f = 0.1$, the LR scheme exhibits somewhat more exchanges than the SSR scheme. The exchange number can be reduced by decreasing f to make the Lagrangian enforcement stronger, at the cost of weakening the strongly centroidal condition.

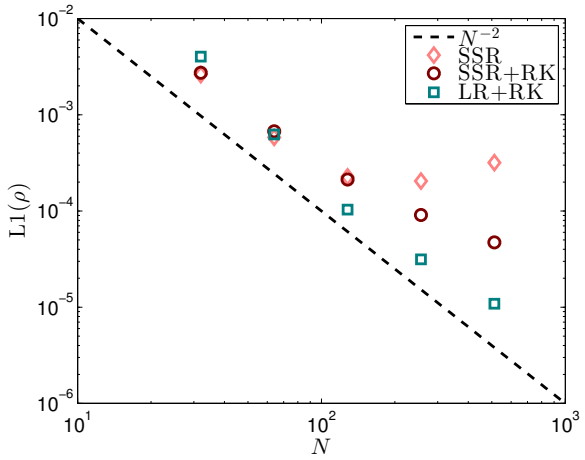

Figure 8. Convergence analysis of the Yee vortex. Proper second-order convergence in the L1 norm is achieved with the LR and the RK time integrator.

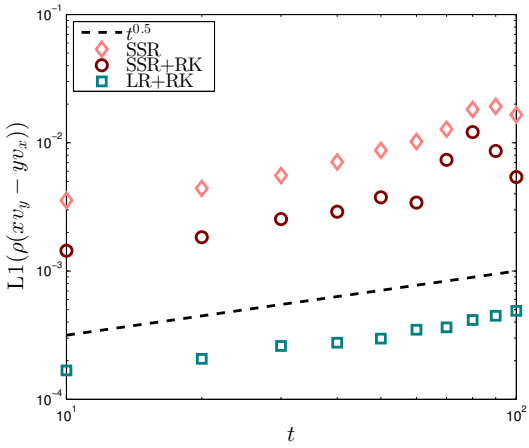

Figure 9. The angular momentum profile error as a function of time. The error is reduced by an order of magnitude with the addition of the LR scheme, and grows in a predictable manner as $t^{0.5}$.

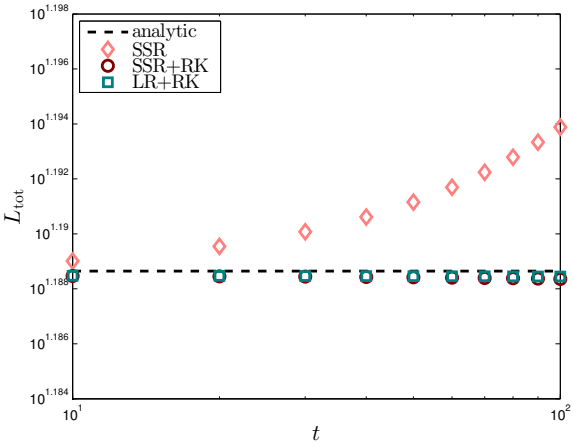

Figure 10. The total angular momentum is well-behaved with the RK time integrator and the LR scheme, but may grow exponentially with the SSR scheme.

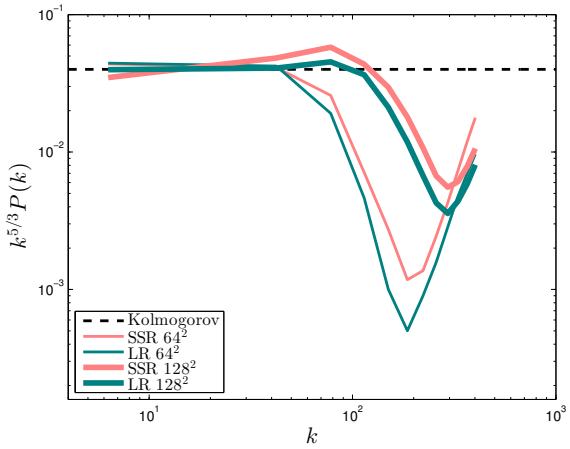

Figure 11. Power-spectrum of driven subsonic turbulence for the two regularization methods. On the smallest spatial scales (large k), the SSR technique shows an excess build-up of power due to mesh noise, which is reduced with the LR scheme.

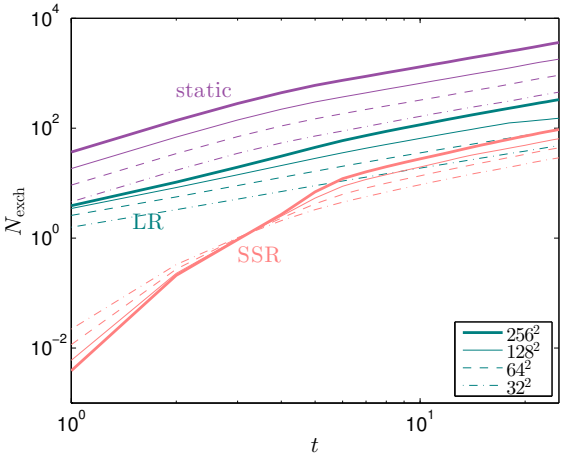

Figure 12. The number of exchanges between cells, $N_{\rm exch}$, that Monte Carlo tracers experience as a function of time in the various turbulent box runs using different cell regularization schemes and at different resolutions. A lower number of exchanges indicates a simulation that is closer to fully-Lagrangian. Using a moving mesh instead of a static mesh reduces the number of exchanges by over an order of magnitude. The LR method, in keeping the mesh centroidal to a high degree, is somewhat less Lagrangian than the SSR scheme.

3.5 Adiabatic jet simulations with KHI

As a test of the new regularization method in an astrophysical context where it is expected to have an impact, we present simulations of heavy, supersonic, adiabatic jets that have a helical mode excited which triggers the KHI, following the setup of Bodo et al. (1998); Micono et al. (2000). This situation is ideal for the study of different phases of the temporal evolution as a function of sound-crossing time. The jet has a surrounding gas density to jet density ratio of $\nu = 0.1$, and a supersonic Mach number of $M = 10$. Our simulations are in 3D and use 5 million cells. In Figure 13, we present the results of the simulation at a point where the KHI has developed and shredded the jet. The LR scheme shows lower level

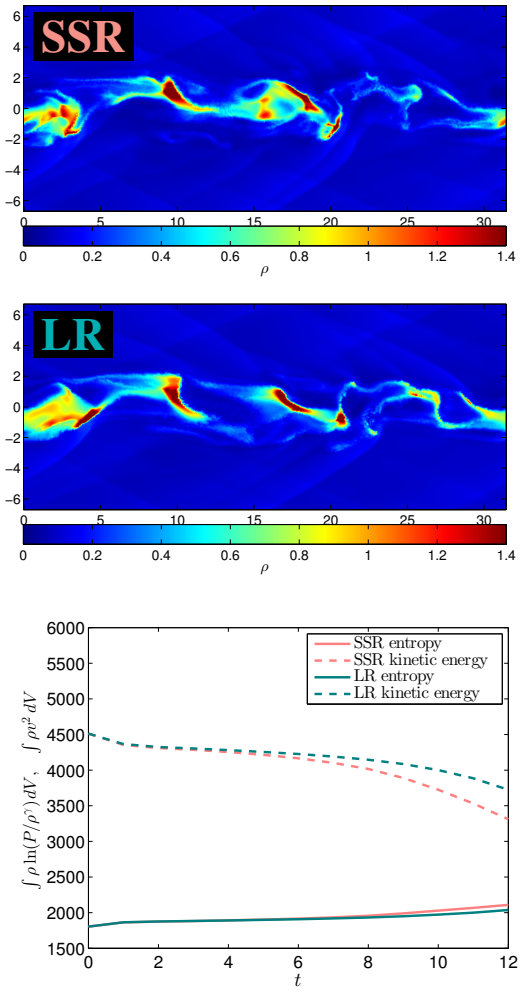

Figure 13. Simulation of an $M = 10$, heavy, adiabatic jet with the two regularization methods. The cross-sections are at time $t = 7$ sound-crossing times. Entropy generation is higher at late times with the SSR scheme than with the LR scheme.

of mesh noise and entropy generation than the SSR technique at late times in the simulation.

3.6 Isolated galaxy formation

Finally, we simulate the formation of an isolated disk galaxy with magnetic fields similar to the Milky Way, following the setup of Pakmor & Springel (2013). The initial gas sphere in the simulation is in hydrostatic equilibrium (without radiation), but collapses due to radiative cooling. The gas has some initial angular momentum, and settles into a dense, rotationally supported disk. Regions in the disc can fragment and are allowed to form stars. In this simulation with collapse, we bias the initial velocities of the mesh generating points by the density gradient term as in Vogelsberger et al. (2012), before applying the Lloyd regularization, in order to closely follow the collapse. We present the results of the simulations under the LR and SSR schemes as well as time evolution of some global properties in Figure 14, and find the results are unaffected by the regularization because mesh noise errors are sub-dominant. The simulations have a mass resolution of $10^6\ M_\odot$.

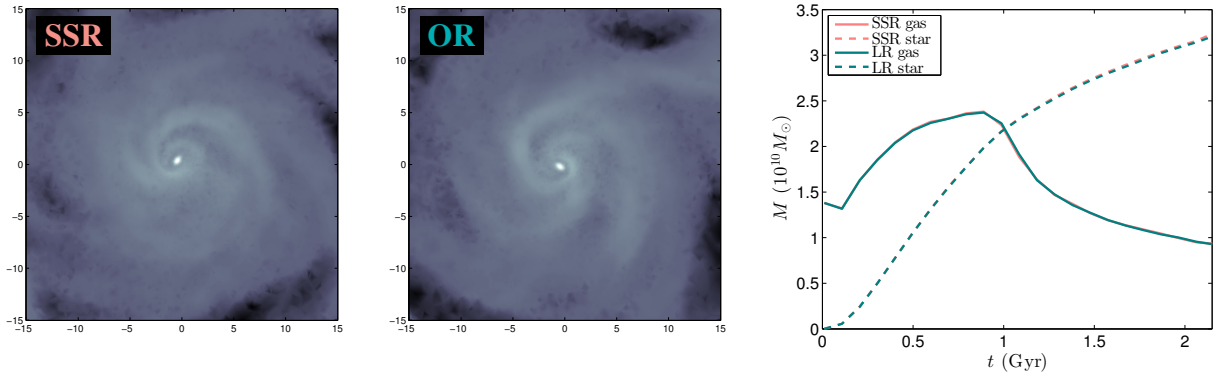

Figure 14. Simulation of the formation of an isolated magnetic disc using the two regularization schemes. The first two panels show a slice of the gas density field, while the third panel shows the time evolution of mass of stars and gas within a 15 kpc radius. Regularization does not affect the global properties of the simulation. The density scale covers $-5 \leq \log_{10} \rho \leq -0.8$.

4 CONCLUDING REMARKS

In summary, we have presented a new regularization scheme, Lloyd Regularization (LR) for moving Voronoi mesh codes that significantly reduces mesh noise and improves convergence and angular momentum conservation. These advantages are gained because the new LR scheme keeps the cells centroidal to a high degree by applying a forward-predicting Lloyd iteration correction to the mesh generating point. The regularization scheme will improve the science applications of moving mesh codes used in astrophysics, particularly in systems where shear flows exist. The LR scheme allows moving mesh codes to capture the physics of fluid instabilities more accurately than earlier methods, which are thought to be important for jet dynamics and gas stripping in galaxies. The correct level of turbulence and entropy generation is also improved with the reduction of mesh noise through this method. The improvements are most relevant for shear flows, and complements the recent moving-mesh improvements for smooth solutions of Pakmor et al. (2015).

ACKNOWLEDGEMENTS

This material is based upon work supported by the National Science Foundation Graduate Research Fellowship under grant no. DGE-1144152 (PM). LH acknowledges support from NASA grant NNX12AC67G and NSF award AST-1312095. SG acknowledges support for program number HST-HF2-51341.001-A provided by NASA through a Hubble Fellowship grant from the STScI, which is operated by the Association of Universities for Research in Astronomy, Incorporated, under NASA contract NAS5-26555. RP acknowledges support by the European Research Council under ERC-StG grant EXAGAL-308037 and by the Klaus Tschira Foundation.

REFERENCES

Bauer A., Springel V., 2012, MNRAS, 423, 2558 1, 3.4
Bodo G., Rossi P., Massaglia S., Ferrari A., Malagoli A., Rosner R., 1998, A&A, 333, 1117 3.5
Duffell P. C., MacFadyen A. I., 2011, ApJS, 197, 15 1
—, 2014, MNRAS, in press, arxiv:1407.7300 1
Gaburov E., Johansen A., Levin Y., 2012, ApJ, 758, 103 1
Genel S., Vogelsberger M., Nelson D., Sijacki D., Springel V., Hernquist L., 2013, MNRAS, 435, 1426 3.4
Genel S. et al., 2014, MNRAS, 445, 175 1
Hopkins P. F., 2014, MNRAS, in press, arxiv:1409.7395 1
McNally C. P., Lyra W., Passy J.-C., 2012, ApJS, 201, 18 3.1
Micono M., Bodo G., Massaglia S., Rossi P., Ferrari A., Rosner R., 2000, A&A, 360, 795 3.5
Mocz P., Vogelsberger M., Hernquist L., 2014, MNRAS, 442, 43 1, 3.2
Mocz P., Vogelsberger M., Sijacki D., Pakmor R., Hernquist L., 2014, MNRAS, 437, 397 1, 3.1, 3.4
Orszag S. A., Tang C.-M., 1979, Journal of Fluid Mechanics, 90, 129 3.2
Pakmor R., Springel V., 2013, MNRAS, 432, 176 3.6
Pakmor R., Springel V., Bauer A., Mocz P., Munoz D. J., Ohlmann S. T., Schaal K., Zhu C., 2015, MNRAS, in press, arxiv:1503.00562 1, 3.3, 4
Sijacki D., Vogelsberger M., Kereš D., Springel V., Hernquist L., 2012, MNRAS, 424, 2999 1
Springel V., 2010, MNRAS, 401, 791 1, 3.1, 3.2
Steinberg E., Yalinewich A., Sari R., Duffell P., 2015, ApJS, 216, 14 1
Toro E. F., 1999, Riemann solvers and numerical methods for fluid dynamics. 1
Vogelsberger M. et al., 2014a, Nat, 509, 177 1
—, 2014b, MNRAS, 444, 1518 1
Vogelsberger M., Sijacki D., Kereš D., Springel V., Hernquist L., 2012, MNRAS, 425, 3024 1, 2, 3.6
Yee H. C., Sandham N. D., Djomehri M. J., 1999, Journal of Computational Physics, 150, 199 3.3
Zhu Q., Hernquist L., Li Y., 2015, ApJ, 800, 6 1

This paper has been typeset from a TEX/ LATEX file prepared by the author.